VALORIZATION OF KAPOK (*CEIBA PENTANDRA* (L.) GAERTN.) PODS FOR MICROCRYSTALLINE CELLULOSE: EXTRACTION AND CHARACTERIZATION

E. K. VYDHEHI, AJMAL THAYYULLATHIL, SUBAIR NADUPARAMBATH and T. M. ANJANA

Post Graduate and Research Department of Chemistry, Government College Madappally, University of Calicut, Vadakara, Kozhikode 673102, Kerala, India
✉ *Corresponding author: E. K. Vydhehi, vaidehiek@gmail.com*

Received January 27, 2025

Kapok (*Ceiba pentandra*) pods – an abundant yet underutilized agricultural waste – were valorized for the first time to produce high-purity microcrystalline cellulose (MCC) through a tailored chemical process involving delignification, alkali treatment, and acid hydrolysis. Unlike prior studies focused on kapok fibers, this work exploits the pods' untapped potential, addressing both waste disposal challenges and the demand for sustainable cellulose sources. Comprehensive characterization confirmed the efficacy of the process: FTIR spectra indicated near-complete removal of lignin and hemicelluloses, while XRD revealed a unique coexistence of cellulose I and II allomorphs, with crystallinity indices escalating from 67.02% in α-cellulose to 72.39% in MCC. Notably, the derived MCC exhibited exceptional properties – a mesoporous structure, which was validated by N_2 sorption and suggested by TEM, ideal for dye adsorption, with enhanced thermal stability, showing decomposition temperature higher than those of α-cellulose and raw pods, and microfibrous morphology with rough surfaces, as revealed by FE-SEM. Further, colloidal stability analysis (zeta potential) and particle size distribution underscored its suitability for nanocomposites. This study pioneers Kapok pods as a low-cost, eco-friendly source of high-performance MCC, offering a dual advantage of waste upcycling and advanced material fabrication for biosorbents and bionanocomposites.

Keywords: kapok pods, lignin, holocellulose, α-cellulose, MCC, composites, adsorbents

INTRODUCTION

Battista and Smith explored the new avenue of microcrystalline cellulose (MCC) in 1955, and the quest for finding the 'inexhaustible treasure', MCC, from various renewable sources continues with unabated zest.[1] Microcrystalline cellulose (MCC) is a purified, partially depolymerized form of cellulose with the molecular formula $(C_6H_{10}O_5)_x$ that occurs as a white, odourless, tasteless, crystalline powder composed of porous particles.[2] MCC is a cellulose derivative with a plethora of versatile industrial applications. The ability of MCC to bulk, disintegrate, bind, and lubricate makes it conducive to its application as an adsorbent, binder, and excipient in the pharmaceutical and cosmetic industry.[3] Approved by the U.S. Food and Drug Administration (FDA), and generally recognized as safe (GRAS),[4] microcrystalline cellulose is a food additive with a multitude of functions in the food industry – as thickening agent, stabilizer, emulsifier, gelling agent, fat substitute, texturizer, suspending agent, and anti-caking agent. In addition, MCC as a reinforcing agent is attracting increasing interest due to its potential advantages, such as renewability, biodegradability, biocompatibility, economic value, non-toxicity, high mechanical properties, and high surface area for bonding with polymer matrices. Furthermore, MCC complies with customizing or modifying chemical species to improve the morphology, thermal, and mechanical properties of the resultant composites.[5] MCC as an eco-friendly filler in food packaging confers enhanced barrier, mechanical, and optical properties, leading to an improvement in the shelf life and freshness of the food products.[6]

Wood and cotton are the preponderant sources of MCC, but it is the need of the hour to find alternative potential sources for the fabrication of MCC.[7] Using agro-industrial by-products reduces the reliance on wood as a feedstock, thus

minimizing deforestation and the carbon footprint. Research focusing on the cascade utilization of lignocellulosic biomass has garnered great impetus worldwide in the context of ever-increasing environmental concerns and the search for sustainable smart materials. The main constituents of lignocellulosic fibers are polysaccharides (cellulose and hemicelluloses) and aromatic polymers (lignin).[8] Cellulose is organized structurally into fibrils, surrounded by a lignin and hemicellulose matrix.[9] MCC can be isolated and purified from lignocellulosic biomass using different methods, such as acid hydrolysis, steam explosion,[10] reactive extrusion[11] or an enzymatic process.[12] The acid hydrolysis is the dominant method due to its simple setup, rapid reaction rates, and mild conditions.[13] Microcrystalline cellulose is conventionally prepared by treating α-cellulose with mineral acids. Several lignocellulosic biomasses that have been researched in the past as potential sources of MCC are pistachio shells,[14] orange peel,[15] walnut shells,[16] olive stones,[17] teff straw,[18] black tea waste,[19] bottle gourd fruit pedicles[20] and waste clothes.[21]

Ceiba pentandra L. Gaertn, commonly referred to as Kekabu or Kapok, is a member of the Malvaceae family.[22] Kapok originates from Southeast Asia and is cultivated in regions such as Southeast Asia, India, Sri Lanka, and tropical America. This tree thrives naturally in humid and sub-humid tropical climates and is known for its drought resistance. In the Western Ghats of India (Kerala, Karnataka and Maharashtra), it is commonly found in forested and semi-urban areas due to favourable, humid, tropical conditions. With its rich cellulose content, kapok fiber is potentially used for manufacturing microcrystalline cellulose.[23] Kapok pods (hulls or pericarpium) from these trees are leathery, ellipsoid, and pendulous capsules.[24] These kapok pods are mass-produced waste generated after the post-harvest processing of kapok fruits and do not have any competing uses. The disposal of the accumulated agricultural kapok pod waste was carried out by open burning, which has a devastating impact on the environment, leading to air pollution and squandering a cellulose resource. Their valorisation is urgent to align with global net-zero carbon commitments. The vastness of this bioresidue over both the semi-urban areas and forests in Kerala, India, prompted its value-added utilization. The global demand for sustainable biomaterials is ever-increasing, yet most production relies on non-sustainable sources.

Researchers have performed studies on the chemical treatment of kapok pods. Cellulase enzymes obtained from selected fungal strains were used to manufacture microcrystalline cellulose from kapok cortex.[25] The hydrochar prepared from kapok pods efficiently removed Rhodamine B dye from aqueous solutions.[26] To the best of our knowledge, no studies have been reported on using kapok pods as the key raw material for the development of MCC via acid hydrolysis. The valorisation of kapok pods in MCC production fosters the principles of the circular economy by converting an agrowaste into a material with a lot of applications. It aligns with the United Nations Sustainable Development Goals, by reducing air pollution, and through combating deforestation and sustainably managing bioresources. This study aims to extract MCC from the immensely underutilized kapok pods through bleaching, alkali, and acid hydrolysis treatments. To determine the efficacy of isolated MCC, physicochemical, surface, and thermal characterization was carried out.

EXPERIMENTAL

Materials

Kapok pods were collected from the Kannavam Reserve Forest (part of the Western Ghats biodiversity hotspot in India). The pods were washed with distilled water to remove dirt and aqueous soluble substances, air dried, ground to a fine powder, and sieved through a mesh. The powder was oven-dried and preserved for future uses. Ethanol, toluene, sodium chlorite, acetic acid, sodium hydroxide, and hydrochloric acid were purchased from Merck. All reagents were of analytical grade and used without purification.

Extraction of α-cellulose from kapok pods

Dewaxing

The process used for the extraction of microcrystalline cellulose was based on a previously described procedure,[27] with slight modifications. Prior to delignification, Soxhlet extraction was employed for the dewaxing process. A 3 g oven-dry sample of kapok pod powder was extracted with 200 mL of a 2:1 ethanol-toluene mixture at a controlled temperature of 80 °C for 6 hours. The dewaxed sample was oven-dried at 100 °C-105 °C for 3-4 hours till a constant weight was obtained.

Bleaching

The dewaxed sample (1 g) was refluxed with 3.0% sodium chlorite (20 mL) at pH adjusted to 5.0 by acetic acid at 80 °C for 2 hours on a vertical shaker with vigorous stirring. The resultant residue was filtered, washed with copious amounts of distilled water till the washings became neutral, and oven-dried at 100 °C-105

°C for 3-4 hours till a constant weight was obtained. The bleaching process was repeated thrice for effective delignification and to procure pristine white fibres of holocellulose.

Extraction of α-cellulose

The dried sample (1 g) of holocellulose was treated with 25 mL of 17.5% NaOH at room temperature in three stages spanning 2 hours to remove hemicelluloses and residual pectin. The mixture was then allowed to stand for 1 hour, after which distilled water was added to adjust the NaOH concentration to 8.3%. The solution was filtered and washed with distilled water and 10% acetic acid. The residue (α-cellulose) was washed again with distilled water several times till the washings became neutral and was dried at 105 °C for 3-4 hours.

Isolation of microcrystalline cellulose (MCC)

The α-cellulose (1 g) was hydrolyzed using a hydrochloric acid solution (2.5N) at 100 °C for 30 min under mechanical stirring, with the ratio of 1:20 pulp over liquor.[18] Afterwards, 50 mL of distilled water was added to the reaction beaker and stirred vigorously to quench the acidic reaction. The resultant mixture was allowed to stand overnight. The MCC obtained was filtered, washed with distilled water till it was chloride-free, and oven-dried for 3 hours at 90 °C. The product obtained after drying was snowy-white in appearance and was preserved for further use. The schematic representation for the extraction of microcrystalline cellulose is illustrated in Figure 1.

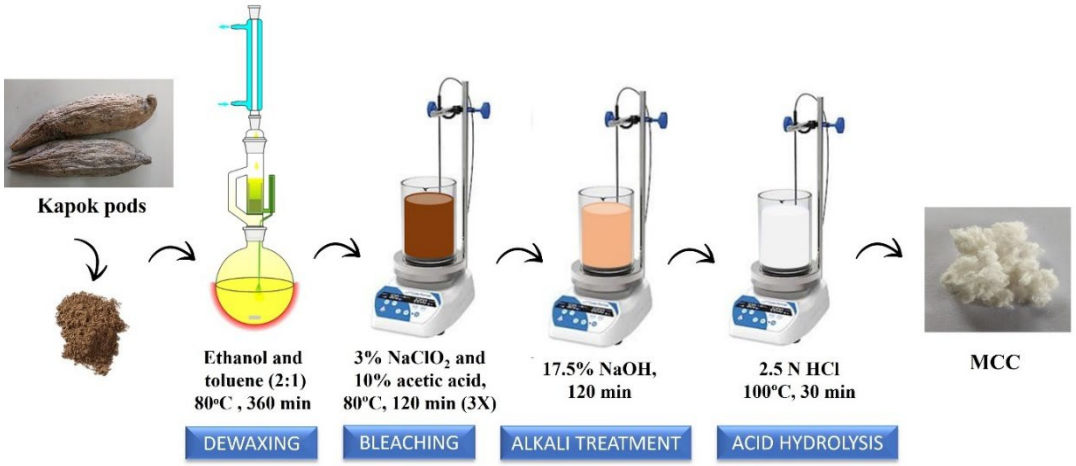

Figure 1: Schematic representation for the extraction of microcrystalline cellulose from kapok pods

Characterization

The products of the successive chemical treatments conducted on kapok pod powder were subjected to various spectral and analytical techniques, as described below.

Morphological studies

The morphologies of kapok pod powder, α-cellulose, and MCC were observed by FE-SEM (Tescan Maia3 Ultra High-Resolution SEM) at a voltage of 10 kV under high vacuum (XMH) to explore the alteration in morphologies, in terms of size and level of smoothness, occurring during the successive chemical treatments. The finely powdered samples were sputter-coated with gold before the morphological assessment to improve conductivity. Micrographs were taken at six different magnifications.

Transmission electron microscopy (TEM) observations were carried out using a Jeol model JEM 2100 at 200 kV. A very diluted (1 mg/mL) kapok MCC aqueous suspension was ultrasonicated in a water bath sonicator, and it was mixed with 1% (w/v) uranyl acetate stain. Then, a drop of the solution was deposited on a carbon-coated copper grid, which was dried and used for imaging.

Particle size distribution analysis and zeta potential

The particle size distribution and zeta (ζ) potential of the kapok-derived microcrystalline cellulose (MCC) colloids were determined using a dynamic light scattering (DLS) nanoparticle analyzer (Horiba SZ-100, Japan) at 25 °C, with deionized water as the dispersing medium. A diode-pumped solid-state (DPSS) laser operating at 532 nm was employed as the light source. Particle size measurements were performed on dilute aqueous suspensions by analyzing the intensity of light scattered at a backscattering angle of 173°. MCC suspensions are not true colloids and they may sediment over time. 0.1–0.2% w/v dispersion of MCC powder in deionized water was sonicated using a probe sonicator for 30 minutes. ~1 mL of the sonicated MCC suspension was transferred into a clean quartz cuvette and three replicate measurements were taken. The Z-average diameter (hydrodynamic diameter), polydispersity index (PDI), zeta potential (mean) and electrophoretic mobility (mean) were recorded.

FTIR analysis

The functional groups and chemical structure of kapok pod powder, α-cellulose, and MCC were analyzed using an FTIR spectrometer (Cary 660, Agilent Technologies, USA). Dry samples (1–2 mg) were mixed with KBr, finely ground for homogeneity, and compressed into pellets. Each pellet was placed in the FTIR sample holder, and spectra were recorded in the range of 4,000–400 cm^{-1}. A background scan was performed before measuring the sample spectra.

X-ray diffraction analysis

The crystalline structure and phase composition of kapok powder, α-cellulose, and MCC were analyzed using an X'pert3 Powder Multi-Purpose X-ray Diffractometer with Cu-Kα radiation (λ = 1.54 Å). Measurements were performed across a 2θ range of 10°-50° with a step size of 0.02° using finely powdered and dried samples. The crystallinity indices (CrI) were calculated using Segal's peak height method:

$$CrI(\%) = \frac{I_{200} - I_{am}}{I_{200}} \times 100 \quad (1)$$

where I_{200} is the maximum crystalline intensity at 2θ~22.50º and I_{am} is the amorphous minimum intensity at 2θ~15º.

The crystallite size was estimated using the Scherrer equation:

$$L = \frac{K\lambda}{\beta \cos\theta} \quad (2)$$

where L is the crystal dimension (in nanometers) perpendicular to the diffracting planes with Miller indices of hkl, λ is the wavelength of X-ray radiation (λ = 1.54Å), Scherrer constant (K = 0.94) represents the shape factor (depends on the shape of the crystallites), $\beta_{1/2}$ is the full width at half maximum (FWHM) of the diffraction peaks, in radians, at a height half-way between background and the peak maximum, and θ is half of the Bragg diffraction peak position (2θ max position).

Thermal stability analysis

The thermal degradation behaviour of kapok pod powder, α-cellulose, and microcrystalline cellulose (MCC) was investigated using simultaneous thermogravimetric and differential thermogravimetric analysis (TGA/DTA) performed on a PerkinElmer STA 8000 thermal analyzer. Approximately 5-10 mg of each pre-dried and finely ground sample was loaded into a platinum crucible and subjected to controlled heating from ambient temperature (25 °C) to 750 °C under a constant nitrogen purge (100 cm^3/min), with a heating rate maintained at 10 °C/min throughout the experiment.

The TGA profiles recorded the mass loss characteristics of the samples as a function of temperature, while the corresponding DTG curves provided the first derivative of the weight loss, enabling precise determination of the decomposition temperatures. This experimental configuration ensured an oxygen-free environment to study the intrinsic thermal stability of the samples without oxidative interference. Three replicate measurements were performed for each sample to ensure reproducibility of the thermal data.

N_2 sorption measurement

To evaluate the adsorption potential of kapok-derived microcrystalline cellulose (MCC), a comprehensive characterization of its porous properties was conducted through N_2 physisorption measurements using a Micromeritics Gemini V 2375 Surface Area Analyzer (USA). Approximately 200 mg of MCC was degassed under vacuum at 80 °C for 12 hours to ensure complete removal of surface contaminants and adsorbed moisture.

The analysis employed high-purity N_2 (99.999%) as the adsorbate at 77 K. The specific surface area was determined by applying the Brunauer-Emmett-Teller (BET) model to the adsorption data within the relative pressure (P/P_0) range of 0-1. Complementary pore characteristics, including pore size distribution and total pore volume, were derived from the Barrett-Joyner-Halenda (BJH) model.

RESULTS AND DISCUSSION

Table 1 depicts the overall compositional analysis of kapok pods. The series of chemical treatments (dewaxing, bleaching, alkali treatment and acid hydrolysis) provided a reasonably good yield (22.58%) of pure microcrystalline cellulose. Therefore, kapok pods can be used as a viable source for the extraction of microcrystalline cellulose, which can be utilized as a cost-effective biosorbent and as a filler for the preparation of composites. From the overall composition, it can be remarked that kapok pods contain higher lignin content (26.68%). The XRD diffractograms of kapok pods reaffirmed the profusion of lignin in its composition. Higher lignin content can be correlated with greater rigidity of kapok pods. However, the raw material was effectively delignified through the three-time vigorous bleaching and alkali treatment, as stated by the FTIR analysis. The higher lignin content can be made advantageous by its proper valorisation.

Morphological analysis

The cell wall is a robust composite material consisting of paracrystalline cellulose fibril aggregates, amorphous hemicelluloses, and branched lignin derived from polyphenols. These components intricately intertwine to create a strong and highly functional vascular structure.[13] Paracrystalline cellulose refers to a semi-ordered non-equilibrium structural state between crystalline and amorphous cellulose. The

mechanical properties, dihedral distribution, hydrogen bonding, chain ordering and potential energy of the paracrystalline cellulose were found to be an intermediary state between the two extremes: crystalline and amorphous cellulose.[28]

Figure 2 shows the FE-SEM micrographs of kapok pod powder, α-cellulose, and kapok MCC, respectively, with different magnifications, revealing the morphological changes that occurred during the successive chemical treatments. Ensuing acid hydrolysis, α-cellulose fibers transfigured into distinct micro-sized cellulose fibers with irregular sizes and shapes. Due to the effects of acid hydrolysis, these microfibers, which were originally bonded by strong hydrogen bonds, evolve into individual microcrystalline fibers. The hydronium ions in the potent acid component of hydrolysis effectively break the glycosidic bonds in cellulose, leading to the formation of irregular microcrystals.[14]

Table 1
Weight % (w/w) of different components isolated from kapok pods

Components	Extractives	Lignin	Holocellulose	Hemicelluloses	α-Cellulose	Ash
Weight (%)	12.63	26.68	55.59	33.01	22.58	5.10

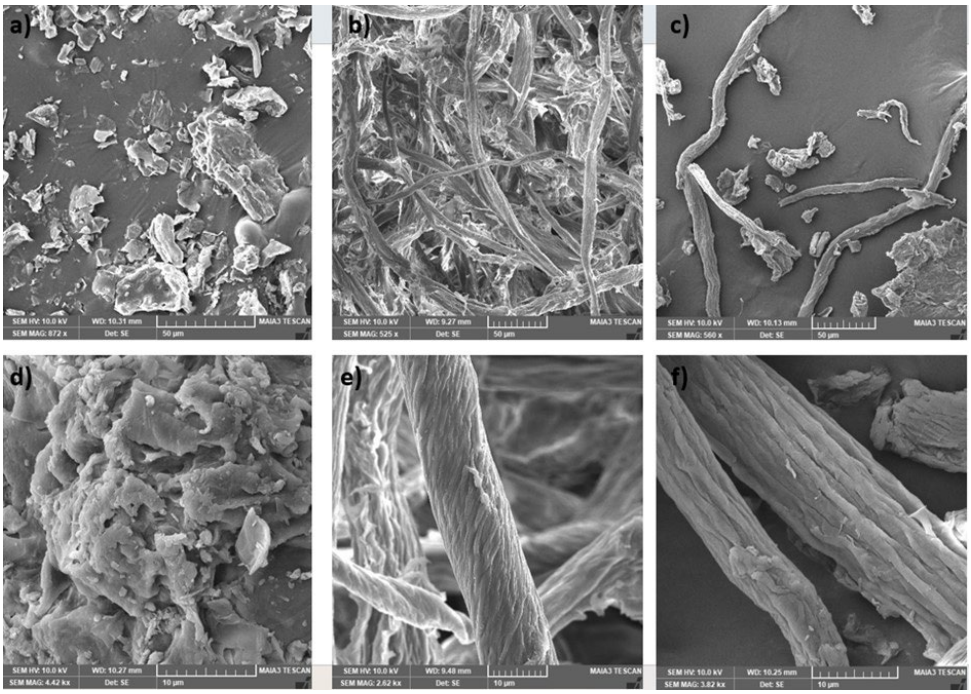

Figure 2: SEM micrographs of (a), (d) kapok pod powder, (b), (e) α-cellulose and (c), (f) MCC at different magnificaton

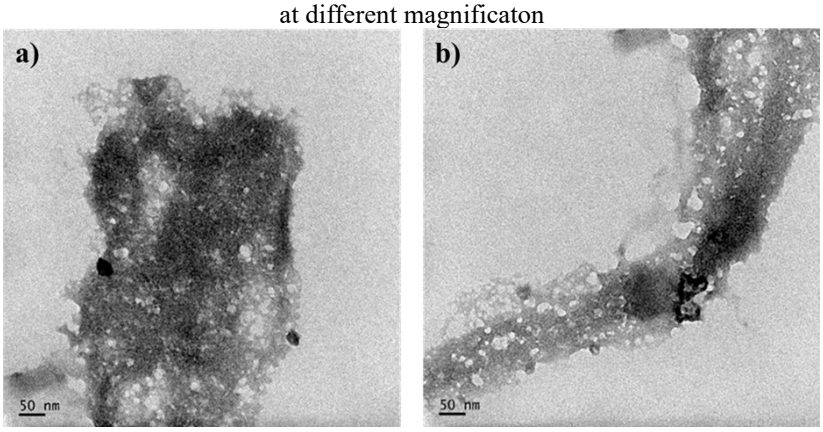

Figure 3: TEM images of kapok MCC

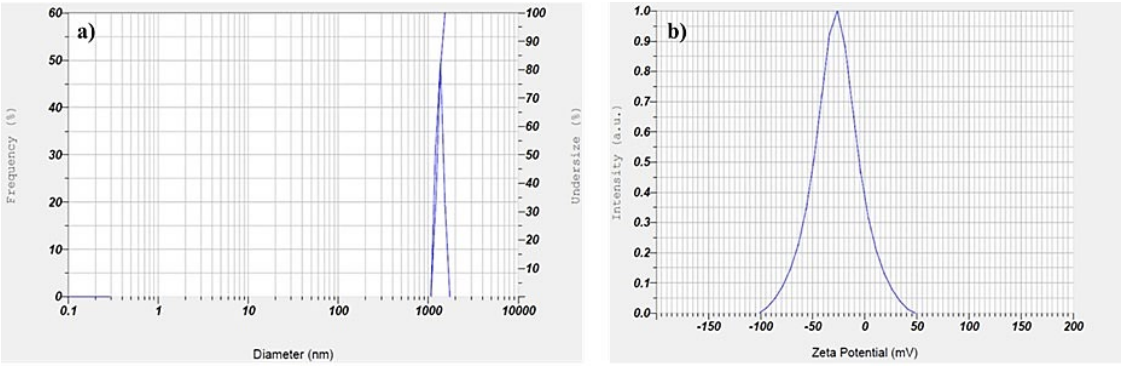

Figure 4: a) DLS plot of MCC and b) Zeta potential curve of MCC

The agglomerated and compact bundle-like structure with irregularities of kapok pod powder implies the presence of cementing materials, lignin and hemicelluloses. Following the delignification and alkaline hydrolysis, the obtained α-cellulose consists of long, individualized, uniform cellulose filaments with smooth surfaces.[29] This observation corroborates with the FTIR spectroscopic evidence of the removal of lignin and hemicelluloses. The kapok MCC particles exhibited short fiber strands with rough and grooved surface morphology. This is explained by the structural disintegration of fibrous strands into smaller-sized microcrystallites during exposure to the HCl treatment, which hydrolytically cleaves the glycosidic bonds of cellulose. The long microfibrillar structure of MCC with a high aspect ratio makes it suitable to be used in the production of high-tensile strength biocomposite products.[30] The acid hydrolysis produced cellulose microfibers with non-uniform diameters ranging between 5-20 µm. This may be due to the aggregation of cellulose during acid treatment, which will prevent uniform acid penetration, leading to partial degradation in some areas and over-etching in others.

Transmission electron micrograph images are shown in Figure 3, revealing distinct morphological features that provide insight into the microstructure of MCC. The dark regions suggest thicker, denser areas, likely representing agglomerated MCC particles. The 2D morphology obtained here from TEM analysis can be suggestive of a potentially porous network.

Particle size distribution analysis and zeta potential

From the particle size distribution of kapok MCC given in Figure 4, the size distribution was monodisperse, and its mean size was calculated to be 1.2678 µm (PDI = 0.367) (SD = 109.2 nm). The polydispersity index (PDI) is a measure of dispersion homogeneity. PDI values range from 0 to 1.0, where values from 0 to 0.3 refer to the highest homogeneity distribution state.[17] The disparity in particle size as observed by SEM and DLS arises from the fact that DLS indicates the hydrodynamic radius of particles dispersed in a solution. Because cellulose molecules are highly hydrophilic, they will swell in water.[31]

Kapok MCC exhibited a relatively high negative zeta potential at about -34.1 mV. The hydroxyl groups present in cellulose are deprotonated, which leads to a moderately negative zeta potential value.[31] The negative values of zeta potential indicate the stability and the possible agglomerating tendency of the particles in a water medium.[32]

FTIR analysis

En bloc, all the samples exhibited a similar absorption pattern, which indicated that all the samples have similar chemical compositions. The FTIR spectrum given in Figure 5 conveniently depicts the minuscule yet momentous compositional changes that have occurred to the kapok pods as a result of the successive chemical treatments. In the oven-dry kapok pod powder, the peak at 1736 cm^{-1} is due to the acetyl group of hemicellulose uronic ester or the carboxylic ester group of the ferulic ring and p-coumaric acid of lignin.[29] The characteristic peak of lignin, caused by the aromatic C=C stretch of the aromatic rings of lignin, is present at 1532 cm^{-1}. Additionally, the presence of lignin can also be related to the band at 1251 cm^{-1}, which is indicative of the elongation of the ether linkages (C–O–C).[33] These peaks diminished in intensity or completely disappeared after delignification and bleaching, elucidating that the chemical treatments could effectively discard hemicelluloses and lignin. The FTIR spectra of the

kapok MCC show absorptions at approximately 892 cm^{-1}, 2896 cm^{-1}, and 3431 cm^{-1}, which are attributed to β-glycosidic linkages between anhydroglucose units in the cellulose, C-H symmetric tensile vibration and -OH stretching, respectively.[34] The peak at approximately 1645 cm^{-1} is due to the adsorbed water. The absorption band located at approximately 1374 cm^{-1} is associated with the bending vibration (wagging) of the CH of cellulose. There is an augmentation in the intensity of the peak at 1429 cm^{-1} attributed to a symmetric CH_2 bending vibration (scissoring) from the kapok pods to MCC. This peak is also known as the "crystallinity band", and the increase in the intensity of this peak showcases the increase in the crystallinity index.[35] The peak at 1058 cm^{-1} indicates asymmetric C–O–C stretching vibrations in the pyranose ring units in the cellulose structure.[36]

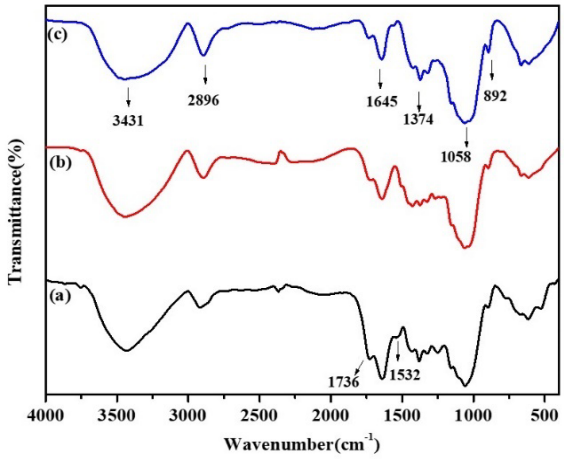

Figure 5: FTIR spectra of a) kapok pods, b) α-cellulose and c) MCC

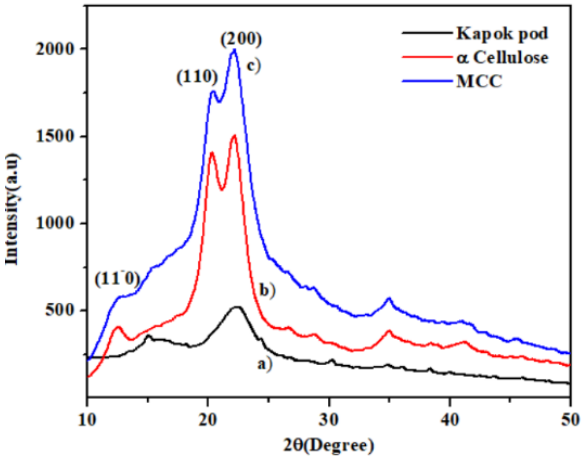

Figure 6: XRD diffractograms of a) kapok pods, b) α-cellulose and c) MCC

X-ray diffraction analysis

X-ray diffraction of the powder sample sheds light on the degree of crystallinity as well as on the kind of polymorphic form in which it exists. The XRD spectra of kapok pod powder, α-cellulose, and MCC are shown in Figure 6.

The kapok pods showed broad diffraction peaks at 2θ = 15° and at 22.3°, similar to sengon wood[36] due to the high content of hemicelluloses and lignin that are naturally present in the amorphous form. After the delignification and alkaline hydrolysis treatment, the α-cellulose and MCC exhibited the pattern of cellulose-II structure with peaks at 12.57° (plane $1\bar{1}0$) at 20.31° (110) and 22.6° (200).[37] The appearance of a doublet in the main peak around 2θ = 22° also confirmed the existence of cellulose II allomorph.[38] This observation alluded to the coexistence of cellulose I and cellulose II allomorphs almost to the same extent ($I_{22.05}/I_{20.32} \sim 1.06$). The value of the ratio greater than unity may be interpreted as an increase in the proportion of cellulose I crystallites to cellulose II crystallites.[39] The partial allomorphic transition of cellulose I to cellulose II structure formation occurred because of the high concentration of sodium hydroxide used during bleaching.[33] The crystallinity indices of α-cellulose and MCC are 67.02% and 72.39%, respectively. The high crystallinity of α-cellulose obtained after delignification and alkaline hydrolysis implies that these processes were highly effective in removing binding components of lignin and hemicelluloses.[40] The enhancement in crystallinity for MCC, to 72.39%, is caused by the ability of hydronium ions to penetrate the more acid-susceptible amorphous region, causing the breakdown of glycosidic bonds, dissolution of the amorphous section, and reorganization in the crystalline cellulose order. Microcrystalline cellulose was considered to have high crystalline structures when the crystallinity index was measured in the range of 55-80%.[41] The benefits of having high crystallinity (>70%) for MCC include a significant increase in chemical and thermal stability and bacteria resistance.[23] Thus, the high crystallinity of kapok MCC makes it as potential load-bearing agent in composite reinforcement applications.[3]

A comparison of the crystallinity index (CI) of kapok pod MCC with MCC derived from other bioresources is consolidated in Table 4. The crystallinity index of kapok pod MCC was higher

than those of MCC derived from rice husk,[32] kapok fibre,[36] pomelo peel,[42] and pistachio shells.[14] The CI of kapok fibres was on par with those of *Conocarpus* fibre[3] and *Washingtonia* fibre.[40] It can be deduced from the above data that there is no direct linear correlation between hydrolysis time and crystallinity index. Some biomass types (*e.g.*, teff straw, *Posidonia*) achieve high crystallinity at short treatment times (30 min), while in some other longer treatments (*e.g.*, pomelo peel at 100 min) can significantly reduce crystallinity. Crystallinity likely depends more on biomass type and treatment conditions. Acid concentration and temperature also influence the outcome.

While kapok fiber yields more cellulose[36] and thereby more MCC, kapok pod-derived MCC exhibits superior crystallinity (72.39%) to that of fiber MCC (68%), making it a functionally advanced material despite slightly lower yields. This trade-off is critical for high-performance applications, justifying the urgency of developing kapok pod MCC.

Table 2
Crystallinity indices of α-cellulose and MCC

Sample	α-cellulose	MCC
Crystallinity index (%)	67.02	72.39

Table 3
Crystallite sizes of MCC planes

Crystallite size perpendicular to each plane L (nm)		
$(1\bar{1}0)$	(110)	(200)
7.03	4.37	4.01

Table 4
Comparison of MCC derived from different biomass sources

Biomass	Treatment method used	Treatment time	Crystallinity index (%)	Refs.
Conocarpus fibre	Acid hydrolysis: 2.5 N HCl at 80 ºC	30 min	72.7	[3]
Teff straw	Acid hydrolysis: 2.5 N HCl at 105 ºC	30 min	85	[18]
Washingtonia fibre	Acid hydrolysis: 2.5 N HCl at 80 ºC	30 min	72.6	[40]
Rice husk	Acid hydrolysis: 2.5 N HCl at 105 ºC	20 min	64.74	[32]
Posidonia oceanica brown algae	Acid hydrolysis: 2.5 N HCl at 100 ºC	30 min	79.5	[48]
Kapok fiber	Acid hydrolysis: 3.5 N HCl at 70 ºC	90 min	67.81	[36]
Pomelo peel	Acid hydrolysis: 6%w/w HCl at 90 ºC	100 min	40.53	[42]
Pistachio shell	Acid hydrolysis: 2.5 N HCl at 105 ºC	45 min	64.94	[14]
Kapok pods	Acid hydrolysis: 2.5 N HCl at 100 ºC	30 min	72.39	This work

Thermal stability analysis

To evaluate the efficiency of the extracted MCC in the production of biocomposites, it is essential to investigate their thermal stability, since biocomposites may have to tolerate extremely high temperatures during the course of their manufacturing stage and in their service.[29] Figure 7 (a-c) shows the TGA curves of the kapok pod, α-cellulose, and MCC. The TGA curves for all the samples, except the kapok pod, show three stages of thermal degradation within the temperature range 30 ºC–750 ºC with different rates and extents. The first stage of degradation at a temperature range of 60–120 ºC, approximately, may be attributed to the evaporation of loosely bound moisture on the surfaces of these materials. The chemisorbed water or the intermolecularly H-bonded water (as apparent from the characteristic peak of FTIR spectra at 1645 cm^{-1}) is found to be given off at around 120 ºC for all the samples.[39] The weight loss during this stage was noted to be 14.09% for kapok pod powder, 9.99% for α-cellulose, and 9.34% for MCC, indicating that kapok pod powder is more hydrophilic than MCC. The amount of sorbed water is proportional to the amorphous region of the sample; thus, the more crystallinity, the less water absorption. The second degradation occurs within a wide range near 200 ºC–360 ºC, owing to decarboxylation, depolymerisation, and decomposition of glycosyl

units, followed by the formation of a charred residue. The final phase is attributed to the breakdown of charred residues and oxidation. In addition, the formation of residual char was relatively low for MCC when compared to kapok pod and α-cellulose. This showcased that the purity of cellulose has been enhanced with the chemical treatment stages.[40]

The DTG curves shown in Figure 8 (a-c) elucidate that the maximal decomposition temperature (T_{max}) increased from kapok pod powder to MCC samples as the thermal stability of fiber samples was enhanced with a higher crystallinity degree. The kapok MCC sample showed the highest T_{max} at 342 ºC, and this suggested kapok MCC is a suitable candidate for use in high-temperature processing applications. The presence of more than three decomposition stages in kapok pod powder is visible in the DTG curve. It may be due to the presence of impurities, which are successfully eliminated in the successive chemical treatments. The degradation peak temperature of kapok pod MCC was lower than that of alfa fibers MCC (351.39 °C)[29]and olive fiber MCC (359.1 °C)[43] using acid hydrolyzed cellulose, and this may be correlated to the lower crystallinity index of kapok pod MCC than that of MCC from alfa fibres (73.62%) and olive fibers (74.2%). Kapok pod MCC contain comparatively more amorphous regions than alfa fibre MCC and olive fibre MCC, and it degrades at lower temperatures due to weaker molecular ordering.

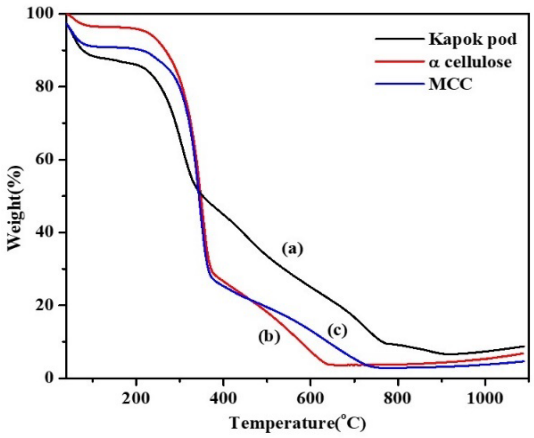

Figure 7: TGA curves of a) kapok pod, b) α-cellulose and c) MCC

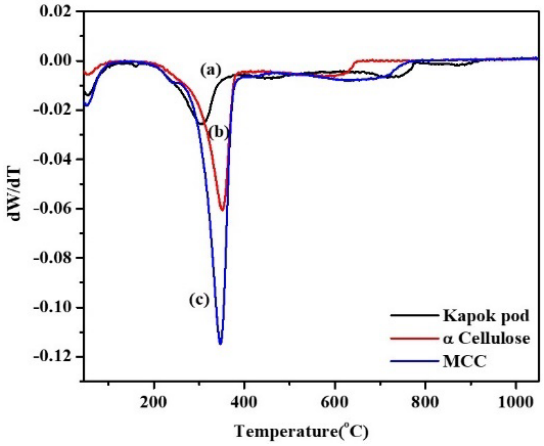

Figure 8: DTG Curve of a) kapok pod, b) α-cellulose and c) MCC

Table 5
Thermal parameters of kapok MCC

Samples	T_{onset} (ºC)[a]	T_{max} (ºC)[b]	Weight of residual char formation (%)[c]
Kapok pod powder	180	300	7.59
α-Cellulose	200	340	5.10
MCC	208	342	3.54

[a] Initial degradation temperature determined by TGA; [b] Peak degradation temperature determined by DTG; [c] Residual weight at 1000 °C determined by TGA

N_2 sorption measurement

As evident from the SEM and TEM micrographs, the kapok MCC wall has a porous structure. To study the pores in detail, the N_2 adsorption measurement was used. Figure 9 shows the N_2 adsorption isotherm of kapok MCC. The range of partial nitrogen vapour pressure (P/P_0) was varied between 0-1 to determine the amount of nitrogen adsorbed. The BET surface area of kapok MCC is 1.70 m^2/g, which is lower than that of sugar palm cellulose (13.18 m^2/g),[44] OPF MCC (5.64 m^2/g)[45] and nearly equal to that of corn cob MCC (1.78 m^2/g).[34] This may be attributed to the bigger particle size than that of sugar palm cellulose and OPF MCC. The surface area is higher than that of porous corncob MCC prepared through the green method (1.43 m^2/g).[46]

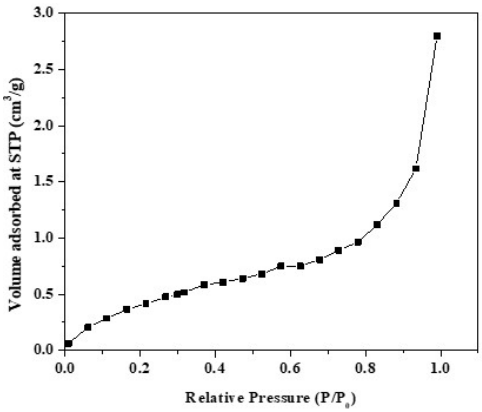

Figure 9: N_2 adsorption isotherm of kapok MCC

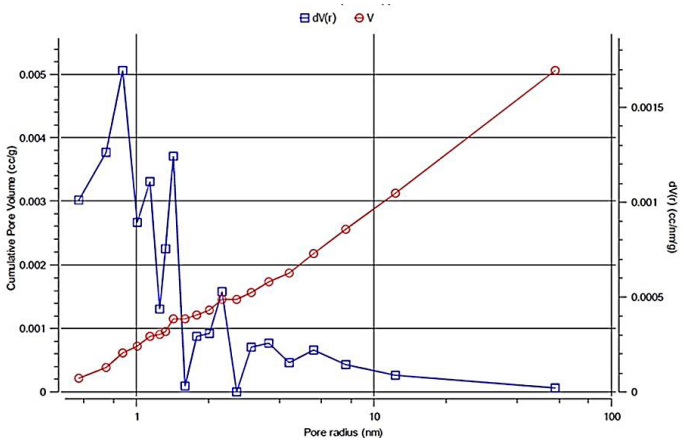

Figure 10: Pore size distribution of kapok MCC calculated by BJH method

Table 6
Pore texture parameters of kapok MCC

S_{BET} (m^2/g)	Pore size (nm)	Pore volume (cm^3/g)
1.70	5.10	4.34×10^{-3}

Figure 10 shows the pore size and pore size distribution of kapok MCC. It is demonstrated that the pore size is mainly located in the mesopore region and partially in the macropore region. The average pore size of kapok MCC, investigated by the BJH method, is 5.10 nm. Based on the average pore diameter, the kapok MCC sample can be classified as mesoporous according to the International Union of Pure and Applied Chemistry, which pores classified as micropores (<2 nm diameter), mesopores (2–50 nm diameter) and macropores (>50 nm diameter).[34] Also, according to IUPAC recommendations, the N_2 adsorption isotherm can be classified as type II, which corroborates with the existence of mesopores and macropores. Moreover, the cumulative pore volume of kapok MCC is 4.34×10^{-3} cm^3/g. The results of those pore properties of kapok MCC are summarized in Table 6. In comparison with microporous materials, mesoporous MCC can act as versatile dye adsorbents because most organic dyes are bulky, and mesopores allow faster, higher-capacity uptake. Moreover, the presence of mesopores allows for easier surface chemical functionalization, which in turn improves the selectivity in adsorption. Mesoporous materials are often easier to regenerate, a crucial aspect in deciding upon its use as adsorbent. Thus, the porosity of MCC may confer a unique application potential, as its modified form can be a porous biosorbent for the fast and efficient removal of low-concentration heavy metal ions and dyes from aqueous solution,[47] and for the preparation of sustained-release tablets.[46]

CONCLUSION

This study is one of the first to comprehensively characterize MCC from kapok pods, highlighting its unique physicochemical properties that differentiate it from MCC obtained from other agricultural residues. The compositional analysis of kapok pods shows that it has a cellulose content of 22.58%. The extracted MCC was subjected to various characterizations. Morphology analyses using FE-SEM reveal the microstructural behaviour of MCC. TEM images are suggestive of the porous structure of MCC. Even though kapok pods contain higher lignin content (26.68%), FTIR analysis of kapok MCC testified to the complete removal of lignin and hemicelluloses. The extracted MCC has a high crystallinity (72.29%), as demonstrated by XRD analysis, and can be recommended as a filler in composites. A comparison of the crystallinity index of kapok-derived MCC with those of MCC derived from other bioresources has been done. Furthermore, thermal stability assessments showed an enhanced decomposition temperature for MCC compared to raw cellulose and kapok pods, highlighting its suitability for high-temperature applications. The porous properties obtained from the N_2 sorption measurement elucidate the potential utilization of MCC as an adsorbent of micropollutants. Different biomass sources yield MCC with unique physicochemical properties, making them suitable for specialized applications. The study is an attempt towards fulfilling the booming demand for sustainable biomaterials.

ACKNOWLEDGMENTS: The authors acknowledge SAIF-MG University, Kottayam, India, for FE-SEM analysis; IIUCNN-MG University, Kottayam, India, for HR-TEM analysis; the School of Chemical Sciences, MG University, Kottayam, for DLS analysis; CSIF, University of Calicut, India, for FT-IR, XRD, and TGA analyses; and CLIF, University of Kerala, Thiruvananthapuram, India, for BET studies.

REFERENCES

[1] S. S. Z. Hindi, *Nanosci. Nanotechnol. Res.*, **4**, 17 (2017), https://doi.org/10.12691/nnr-4-1-3

[2] M. Beroual, L. Boumaza, O. Mehelli, D. Trache, A. F. Tarchoun *et al*., *J. Polym. Environ*., **29**, 130 (2021), https://doi.org/10.1007/s10924-020-01858-w

[3] H. Fouad, L. K. Kian, M. Jawaid, M. D. Alotaibi, O. Y. Alothman *et al*., *Polymers*, **12**, 2926 (2020), https://doi.org/10.3390/polym12122926

[4] J. N. Atindana, M. Chen, H. D. Goff, F. Zhong, H. R. Sharif *et al*., *Carbohyd. Polym*., **172**, 159 (2017), https://doi.org/10.1016/j.carbpol.2017.04.021

[5] G. Lupidi, G. Pastore, E. Marcantoni and S. Gabrielli, *Molecules*, **28**, 2009 (2023), https://doi.org/10.3390/molecules28052009

[6] D. Hermawan, T. K. Lai, S. J. Jafarzadeh, D. A. Gopakumar, M. Hasan *et al*., *BioResources*, **14**, 3389 (2019), http://dx.doi.org/10.15376/biores.14.2.3389-3410

[7] D. Trache, M. H. Hussin, C. T. H. Chuin, S. Sabar, M. R. N. Fazita *et al*., *Int. J. Biol. Macromol*., **93**, 789 (2016), https://doi.org/10.1016/j.ijbiomac.2016.09.056

[8] S. Suzuki, Y. Hamano, N. Wada and K. Takahashi, *ACS Omega*, **8**, 18582 (2023), https://doi.org/10.1021/acsomega.3c00369

[9] F. I. Ditzel, E. Prestes, B. M. Carvalho, I. M. Demiate and L. A. Pinheiro, *Carbohyd. Polym*., **157**, 1577 (2017), https://doi.org/10.1016/j.carbpol.2016.11.036

[10] A. Solikhin, Y. S. Hadi, M. Y. Massijaya and S. Nikmatin, *Waste Biomass Valor*., **10**, 275 (2019), https://doi.org/10.1007/s12649-017-0066-z

[11] A. Merci, A. Urbano, M. V. E. Grossmann, C. A. Tischer and S. Mali, *Food Res. Int*., **73**, 38 (2015), https://doi.org/10.1016/j.foodres.2015.03.020

[12] Y. P. I. Lestari, H. Suryadi, Mirajunnisa, W. Mangunwardoyo, Sutriyo *et al*., *Int. J. Pharm. Pharm. Sci*., **12**, 7 (2020), https://doi.org/10.22159/ijpps.2020v12i3.36468

[13] N. Y. A. Thabit, A. A. Judeh, A. S. Hakeem, A. U. Hamid, Y. Umar *et al*., *Int. J. Biol. Macromol*., **155**, 730 (2020), https://doi.org/10.1016/j.ijbiomac.2020.03.255

[14] S. Y. Park, H. L. Kim and J. Y. Her, *Carbohyd. Polym. Tech*., **7**, 100423 (2024), https://doi.org/10.1016/j.carpta.2024.100423

[15] S. Sohni, S. Begum, R. Hashim, S. B. Khan, F. Mazhar *et al*., *Bioresour. Technol. Rep*., **25**, 101731 (2024), https://doi.org/10.1016/j.biteb.2023.101731

[16] A. C. Khorasani and P. R. Satvati, *Int. J. Biol. Macromol*., **256**, 128432 (2024), https://doi.org/10.1016/j.ijbiomac.2023.128432

[17] M. S. Hasanin, N. Kassem and M. L. Hassan, *Biomass Convers. Biorefin*., **13**, 5015 (2023), https://doi.org/10.1007/s13399-021-01423-y

[18] M. Getachew, T. Gabriel, A. Belete and T. G. Mariam, *J. Nat. Fiber*., **20**, 2245565 (2023), https://doi.org/10.1080/15440478.2023.2245565

[19] B. Debnath, P. Duarah and M. K. Purkait, *Int. J. Biol. Macromol*., **244**, 125354 (2023), https://doi.org/10.1016/j.ijbiomac.2023.125354

[20] M. Achor, Y. J. Oyeniyi and A. Yahaya, *J. Appl. Pharm. Sci*., **4**, 57 (2014), https://dx.doi.org/10.7324/JAPS.2014.40109

[21] S. Singhal, S. Agarwal, A. Kumar, V. Kumar, S. K. Prajapathi *et al*., *J. Polym. Environ*., **31**, 358 (2023), https://doi.org/10.1007/s10924-022-02609-9

[22] J. Baraniak and M. K. Dobrowolska, *J. Nat. Fiber.*, **20**, 2192542 (2023), https://doi.org/10.1080/15440478.2023.2192542
[23] M. A. Mohamed, W. N. W. Salleh, J. Jaafar, A. F. Ismail, M. A. Mutalib *et al*., *Carbohyd. Polym.*, **157**, 1892 (2017), https://doi.org/10.1016/j.carbpol.2016.11.078
[24] P. Sivakumar, S. Sindhanaiselvan, N. N. Gandhi, S. S. Devi and S. Ranganathan, *Fuel*, **103**, 693 (2013), https://doi.org/10.1016/j.fuel.2012.06.029
[25] Mi'rajunnisa, H. Suryadi, Sutriyo and Y. P. I. Lestari, *Sci. Technol. Indonesia*, **8**, 227 (2023), https://doi.org/10.26554/sti.2023.8.2.227-234
[26] K. C. Vasconcelos, S. G. Alencar, A. B. Ferro, L. F. A. M. Oliveira, E. J. S. Fonseca *et al*., *Sep. Purif. Technol.*, **326**, 124787 (2023), https://doi.org/10.1016/j.seppur.2023.124787
[27] S. Naduparambath and E. Purushothaman, *Cellulose*, **23**, 1803 (2016), https://doi.org/10.1007/s10570-016-0904-3
[28] J. L. Bregado, A. R. Secchi, F. W. Tavares, D. de Sousa Rodrigues, R. Gambetta *et al*., *Fluid Phase Equilibr.*, **491**, 56 (2019), https://doi.org/10.1016/j.fluid.2019.03.011
[29] D. Trache, A. Donnot, K. Khimeche, R. Benelmir and N. Brosse, *Carbohyd. Polym.*, **104**, 223 (2014), https://doi.org/10.1016/j.carbpol.2014.01.058
[30] M. Rasheed, M. Jawaid, Z. Karim and L. C. Abdullah, *Molecules*, **25**, 2824 (2020), https://doi.org/10.3390/molecules25122824
[31] M. Adsul, S. K. Soni, S. K. Bhargava and V. Bansal, *Biomacromolecules*, **13**, 2890 (2012), https://doi.org/10.1021/bm3009022
[32] K. Bhandari, S. Roy Maulik and A. R. Bhattacharyya, *J. Inst. Eng. India Ser. E*, **101**, 99 (2020), https://doi.org/10.1007/s40034-020-00160-7
[33] A. P. Travalini, E. Prestes, L. A. Pinheiro and I. M. Demiate, *J. Polym. Environ.*, **26**, 789 (2018), https://doi.org/10.1007/s10924-017-0983-8
[34] X. Shao, J. Wang, Z. Liu, N. Hu, M. Liu *et al*., *Ind. Crop. Prod.*, **151**, 112457 (2020), https://doi.org/10.1016/j.indcrop.2020.112457
[35] T. Zhao, Z. Chen, X. Lin, Z. Ren, B. Li *et al*., *Carbohyd. Polym.*, **184**, 164 (2018), https://doi.org/10.1016/j.carbpol.2017.12.024
[36] R. Abdullah, D. Astira, U. Zulfiani, A. R. Widyanto, A. R. P. Hidayat *et al*., *Bioresour. Technol. Rep.*, **25**, 101728 (2024), https://doi.org/10.1016/j.biteb.2023.101728
[37] J. Li, Z. Wang, P. Wang, J. Tian, T. Liu *et al*., *Int. J. Biol. Macromol.*, **258**, 128936 (2024), https://doi.org/10.1016/j.ijbiomac.2023.128936
[38] T. Gabriel, A. Belete, G. Hause, R. H. H. Neubert and T. Gebre-Mariam, *Cellulose Chem. Technol.*, **56**, 495 (2022), https://doi.org/10.35812/CelluloseChemTechnol.2022.56.42
[39] A. Mandal and D. Chakrabarty, *Carbohyd. Polym.*, **86**, 1291 (2011), https://doi.org/10.1016/j.carbpol.2011.06.030
[40] N. Azum, M. Jawaid, L. K. Kian, A. Khan and M. M. Alotaibi, *Polymers*, **13**, 3030 (2021), https://doi.org/10.3390/polym13183030
[41] M. K. M. Haafiz, S. J. Eichhorn, A. Hassan and M. Jawaid, *Carbohyd. Polym.*, **93**, 628 (2013), https://doi.org/10.1016/j.carbpol.2013.01.035
[42] Y. Liu, A. Liu, S. A. Ibrahim, H. Yang and W. Huang, *Int. J. Biol. Macromol.*, **111**, 717 (2018), https://doi.org/10.1016/j.ijbiomac.2018.01.098
[43] L. K. Kian, N. Saba, M. Jawaid and H. Fouad, *Int. J. Biol. Macromol.*, **156**, 347 (2020), https://doi.org/10.1016/j.ijbiomac.2020.04.015
[44] R. A. Ilyas, S. M. Sapuan and M. R. Ishak, *Carbohyd. Polym.*, **181**, 1038 (2018), https://doi.org/10.1016/j.carbpol.2017.11.045
[45] M. H. Hussin, N. A. Pohan, Z. N. Garba, M. J. Kassim, A. A. Rahim *et al*., *Int. J. Biol. Macromol.*, **92**, 11 (2016), https://doi.org/10.1016/j.ijbiomac.2016.06.094
[46] J. Wang, R. Zhang, C. Quan, X. Shao, N Hu *et al*., *Cellulose*, **29**, 7125 (2022), https://doi.org/10.1007/s10570-022-04724-1
[47] J. Cao, D. Fei, X Tian, Y Zhu, S Wang *et al*., *Cellulose*, **24**, 5565 (2017), https://doi.org/10.1007/s10570-017-1504-6
[48] A. F. Tarchoun, D. Trache and T. M. Klapötke, *Int. J. Biol. Macromol.*, **138**, 837 (2019), https://doi.org/10.1016/j.ijbiomac.2019.07.176